Design and Performance of a Miniature Radar L-Band Transceiver

D. McWatters,[1] D. Price,[2] and W. Edelstein[1]

Radar electronics developed for past JPL space missions historically had been custom designed and as such, given budgetary, time, and risk constraints, had not been optimized for maximum flexibility or miniaturization. To help reduce cost and risk of future radar missions, a "generic" radar module was conceived. The module includes a 1.25-GHz (L-band) transceiver and incorporates miniature high-density packaging of integrated circuits in die/chip form. The technology challenges include overcoming the effect of miniaturization and high packaging density to achieve the performance, reliability, and environmental ruggedness required for space missions. The module was chosen to have representative (generic) functionality most likely required from an L-band radar. For very large aperture phased-array spaceborne radar missions, the large dimensions of the array suggest the benefit of distributing the radar electronics into the antenna array. For such applications, this technology is essential in order to bring down the cost, mass, and power of the radar electronics module replicated in each panel of the array. For smaller sized arrays, a single module can be combined with the central radar controller and still provide the benefits of configuration flexibility, low power, and low mass. We present the design approach for the radar electronics module and the test results for its radio frequency (RF) portion: a miniature, low-power, radiation-hard L-band transceiver.

I. Introduction

A miniaturized radar electronics module (REM) is being developed with the intent to fill the role of a "generic" radar electronics module that can support both a large phased-array system with distributed electronics and a smaller phased-array system with centrally located electronics. The REM contains all of the functionality required for a 1.25-GHz (L-band) radar and can also serve as the back end for a higher-frequency radar system. The key functions of the REM include signal generation, frequency translation, amplification, detection, data handling, and radar control and timing. The REM drives the transmit/receive (T/R) modules located in the antenna and interfaces with the data storage system. The functional elements of the radar electronics module are shown in Fig. 1. An arbitrary waveform generator with its associated logic and digital-to-analog converter (DAC) generates the

[1] Radar Science and Engineering Section.

[2] Communications Ground Systems Section.

The research described in this publication was carried out by the Jet Propulsion Laboratory, California Institute of Technology, under a contract with the National Aeronautics and Space Administration.

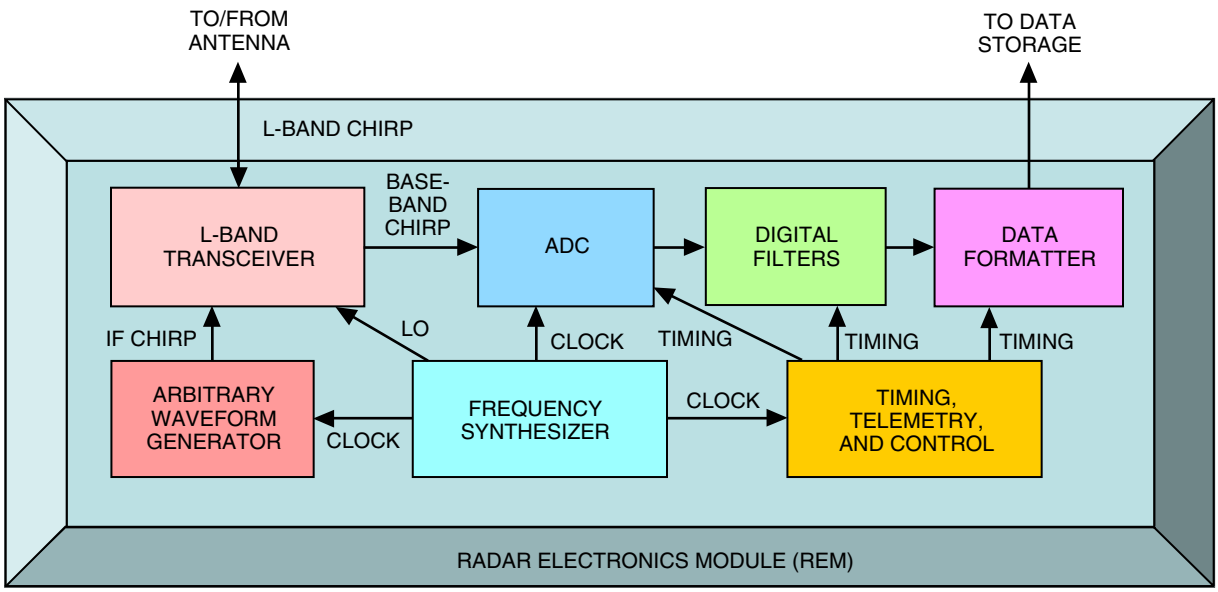

Fig. 1. Radar electronics module functional elements.

linear frequency modulated (FM) chirp waveform. The L-band transceiver includes the radio frequency (RF)–intermediate frequency (IF) downconverter chain and the IF–RF upconverter chain. The frequency synthesizer produces the local oscillators used for frequency conversion and the clocks for the chirp generation, the digitizer (analog-to-digital converter), and the control and timing unit. Digital functions include command, timing and telemetry, analog-to-digital converter (ADC), digital filters, and high-rate data framer/serializer for the high-speed science data interface. A key feature of the REM architecture is digital filtering. Digital filters provide consistent and temperature-independent performance, which is particularly important when the REM is distributed throughout a large array. Digital filtering also enables selection between multiple filter parameters as required by the different operating modes of the radar. After digital filtering, the data will be decimated appropriately in order to minimize the data rate out of the panel. Several components of the radar electronics module are under development. In this article, the design and results of the first component developed, the L-band transceiver, are presented.

II. L-Band Transceiver Design

A set of requirements consistent with several anticipated radar missions was collected for the radar electronics module, and a detailed block diagram was developed, as shown in Fig. 2. The key requirements for each functional block were derived and the interfaces defined. They include the transceiver, digital filters, chirp generator (CG), frequency synthesizer, digital timing and control, which includes pulse repetition frequency (PRF), and data take (DT) timing generation. The digital electronics unit is implemented using field programmable gate array (FPGA) technology. Detailed design of several of the components followed. The focus of this article is to present the work done on the RF portion of the module (i.e., the L-band transceiver).

The functionality of the L-band transceiver (the RF portion of the REM) is shown in Fig. 3. The L-band transceiver includes upconversion from IF to L-band and downconversion from L-band to baseband. T/R switches diplex the transmit and receive signals such that a single feed to the antenna can be used. These T/R switches also enable a calibration signal to be injected into the receiver chain for a built-in-test (BITE) capability. Components were selected according to the following guidelines, listed in order of decreasing priority: radiation hardness (i.e., GaAs or related technology), small size, and low power. All of the RF components are radiation hard. The noise figure (NF) was optimized to the extent

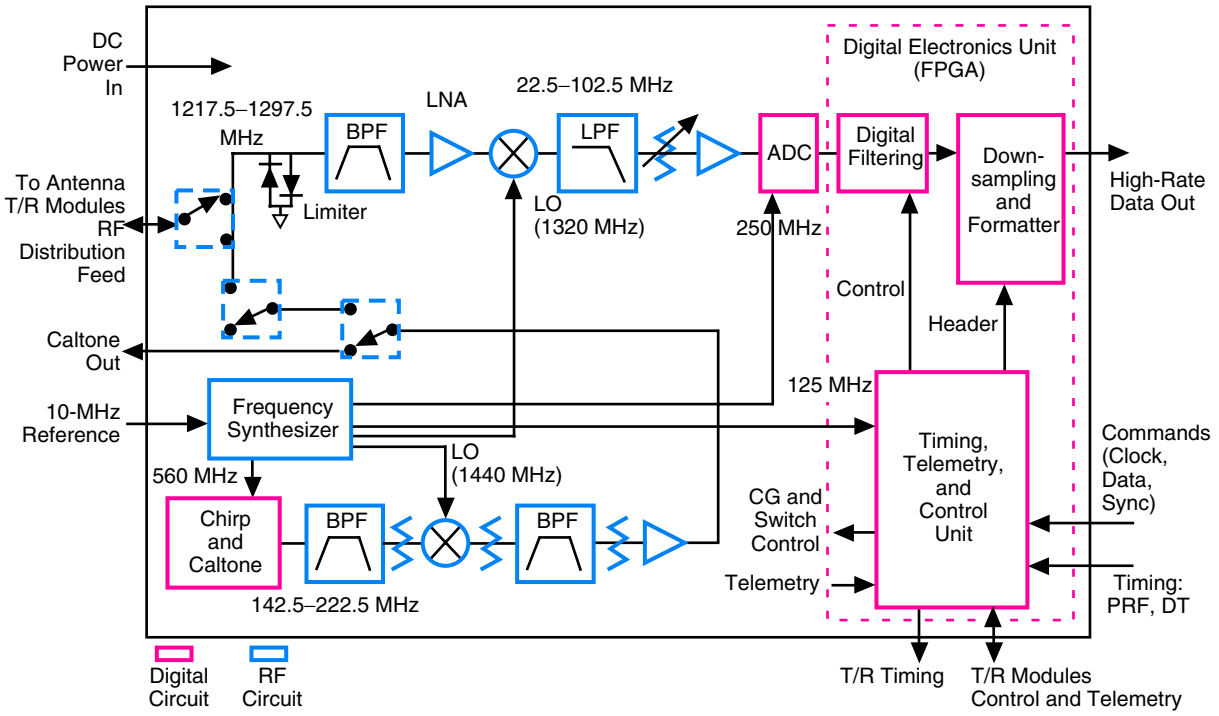

Fig. 2. Radar electronics module block diagram.

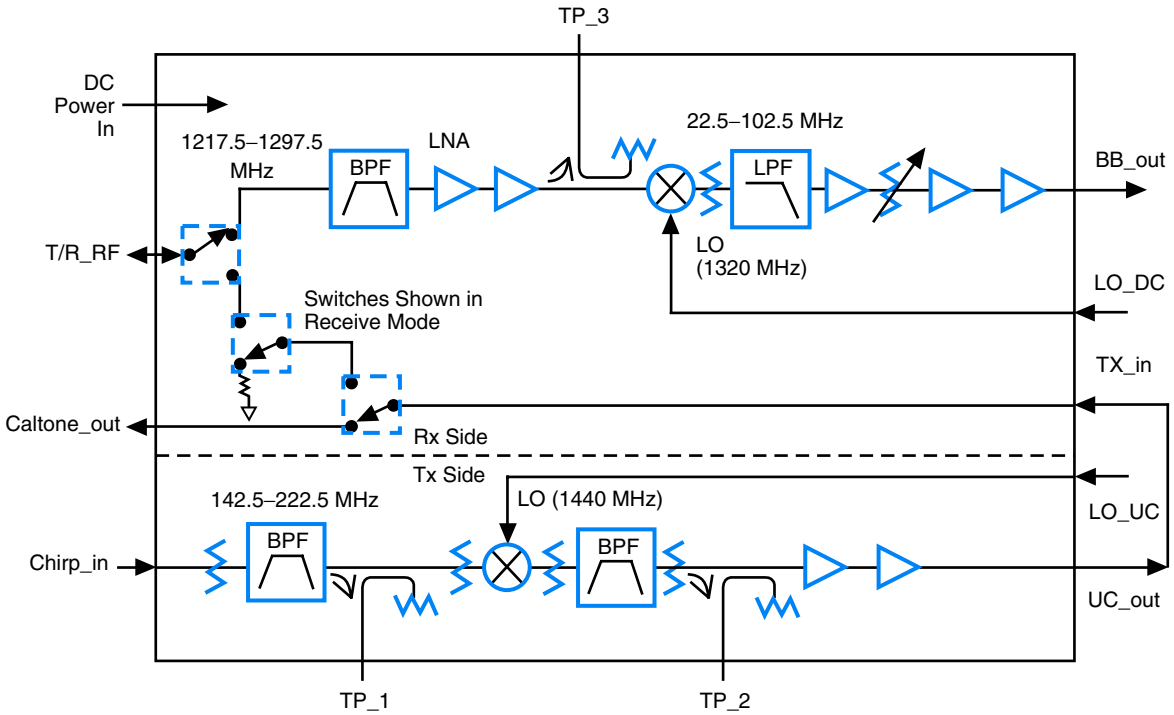

Fig. 3. Miniature radar L-band transceiver module block diagram.
This is the RF portion of the REM shown in Fig. 2.

that an amplifier with NF $<$ 2 dB was selected, but the front-end switches were selected for their good isolation and acceptable loss. The low-noise amplifier (LNA) also has a sufficiently high intercept point to avoid saturation when configured in the back end of the system. The filter specifications were designed to minimize their size, thus placing the downconverted frequency band further offset from DC. This was an acceptable trade-off since the digitizer bandwidth was still realizable with commercial devices and the decimation performed by the digital filters would eliminate the excess bandwidth. The receiver RF bandpass filter (BPF) was chosen to be placed in front of the LNA in order to limit radio frequency interference (RFI). If another filter is placed just before the mixer, the wideband noise of the LNA would not fold into the band, thus decreasing the noise figure. However, this image-rejection filter requires high selectivity and can be large and lossy. For this implementation, the decision was made to use only one RF filter in the receiver and to place it in front of the LNA, thus compromising noise figure but minimizing size and providing input protection from RFI. Since the L-band transceiver interfaces with a low-noise front-end T/R module, this was a reasonable trade to make, without compromising the total receiver noise figure. A programmable attenuator was incorporated to provide adequate dynamic range in the event that the terrain echo amplitude varies significantly. Care was taken to minimize the part count and part types. The amplifiers and mixer used in the upconverter also were used in the downconverter, thus minimizing the cost of parts upscreening to qualify for a space-flight environment.

A. Frequency Conversion Scheme

For an RF band of 1217.5 to 1297.5 MHz (L-band), we chose to produce an intermediate frequency chirp of 142.5 to 222.5 MHz and upconvert it with a local oscillator (LO) of 1440 MHz (thus inverting the spectrum). Using this high-side LO mixing scheme produces no mixing intermodulation products in the L-band chirp passband. In the receive chain, it is desirable to avoid requiring very sharp filters since they are more sensitive to phase versus temperature variations, which would pose a problem for a large array of panels or for high-stability radars. The L-band filter does not need to be very steep, and its purpose is only to limit possible interference and noise into the receiver.

With an LO of 1320 MHz (again inverting the spectrum), the resulting baseband frequency range of 22.5 to 102.5 MHz is to be digitized at 240 megasamples/s. Baseband conversion leads to 2×2, 3×3, 4×4, etc., intermodulation products. However, since the input RF signal level into the downconverter mixer is quite low, the intermodulation products should be sufficiently low. Should there be leakage between the two LO frequencies, their beat frequency would be outside the band of interest. The high oversampling ratio enables the actual band shape to be determined by digital filters, whereas the lowpass filter (LPF) after the mixer is only required to filter the mixing image and reduce the noise into the digitizer.

B. Package Design

The L-band transceiver consists of a mixture of device technologies. The RF integrated circuits were obtained in packaged or bare die form while other components, such as the filters, are much larger. Analog circuitry was separated from digital circuitry in order to minimize noise coupling. The packaging approach was to populate different functions in separate cavities in the module, connecting them through the walls with filtered connections only. This approach provides shielding from noise leakage. Thus, the receive chain (downconverter), transmit chain (upconverter), and control and power supply functions were each in separate cavities of the housing. The active RF components (e.g., amplifiers) are on one side of the module while the passive RF components (e.g., attenuators, filters), control, and power circuits are at the opposite side. The RF functional blocks were further separated into individual substrates and cavities, separated according to frequency. The RF circuit board material is Rogers 4003 except for the RF switches, which are bare die wire bonded to alumina substrate. The control and DC power interface functions are implemented on one epoxy glass printed circuit board. The mass of the L-band transceiver is 270 grams. Photographs of the L-band transceiver module are shown in Fig. 4.

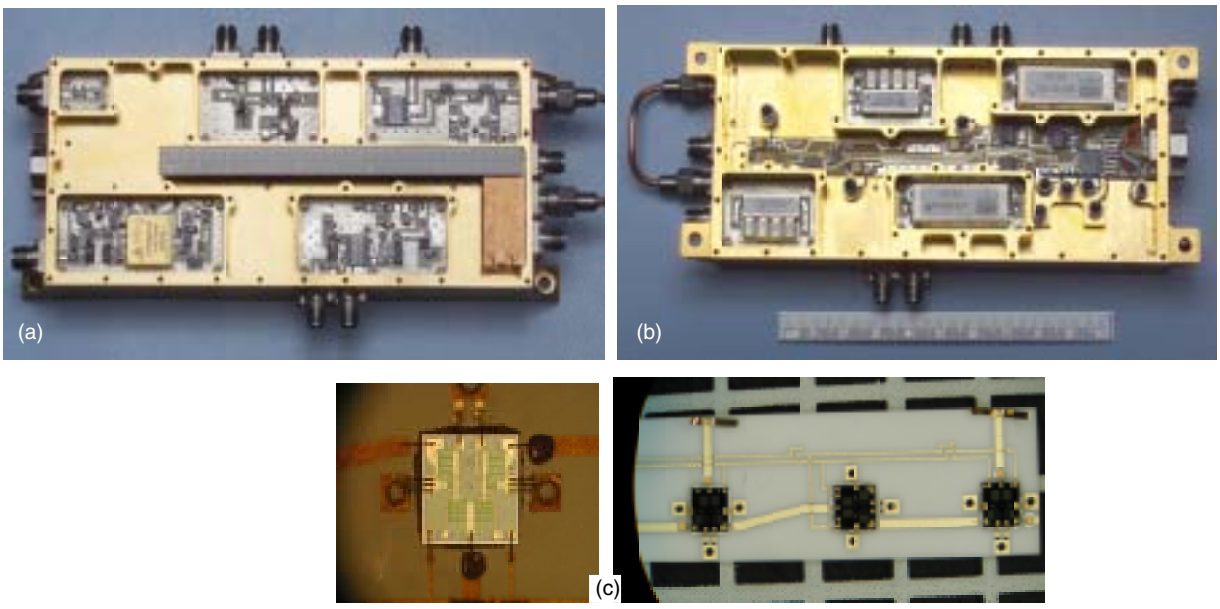

Fig. 4. Uncovered L-band transceiver module: (a) top view (active components), (b) bottom view (filters and control), and (c) close-up views of the packaging of individual switch die circuitry.

III. Test Results

The technology readiness level (TRL) of the L-band transceiver is 5. The module was built and tested in a laboratory environment. The results are presented in the following subsections.

A. Frequency Response

Deviation from the best linear fit in amplitude and deviation from the best quadratic fit for phase contribute to the integrated side lobe ratio (ISLR) of the processed return echo [1]. The passband ripple, out-of-band rejection, and amplitude and phase linearity over frequency were measured on the L-band transceiver module. The up-/down-converter easily meets requirements for amplitude deviation from the best linear fit as well as for phase deviation from the best quadratic fit. Figures 5 through 8 are examples of individual sections of the up-/down-converter that were measured using a network analyzer. From these data, the amplitude/phase deviation of the frequency response was calculated (and noted on the plots). Table 1 is a summary of the frequency response parameters measured using a spectrum analyzer. Receiver passband ripple can be improved by incorporating matching networks between the active components in the chain.

B. Isolation

Isolation between transmit and receive electronics is an important parameter. Poor isolation can result in saturating or even damaging the receiver. Signal leakage also can reduce the ability to calibrate the system. Table 2 shows the results of an isolation test, where a tone was input to the chirp_in port, while the module was in receive mode (i.e., the tone was routed to the caltone_out port while the T/R_RF port was switched to the receive path). The T/R_RF port was terminated into 50 ohms. In this mode, the caltone leakage from the caltone_out port into the receiver competes with the caltone embedded in the radar received signal, coming from the antenna T/R modules. In this configuration, we achieved excellent isolation of close to 100 dB between the caltone_out port and the T/R_RF input to the receiver.

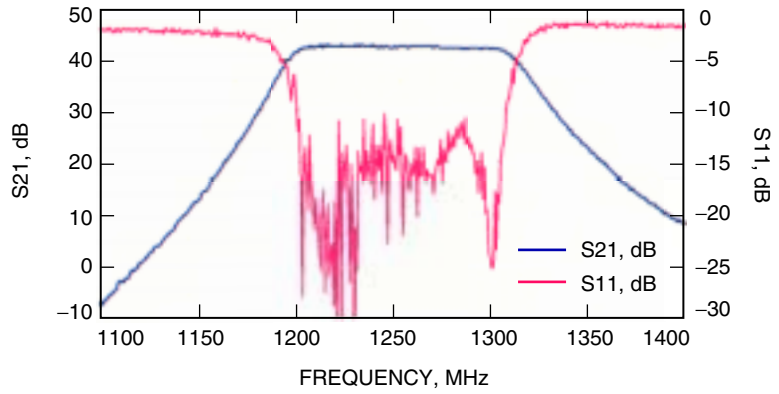

Fig. 5. Input return loss and gain of the downconverter RF section.

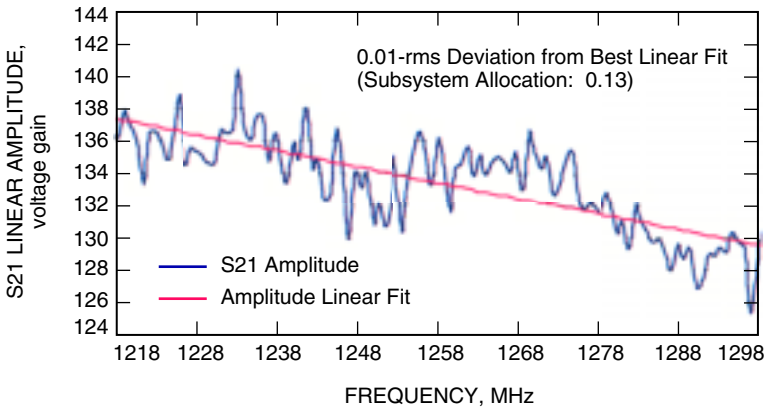

Fig. 6. Amplitude linearity of the downconverter RF section.

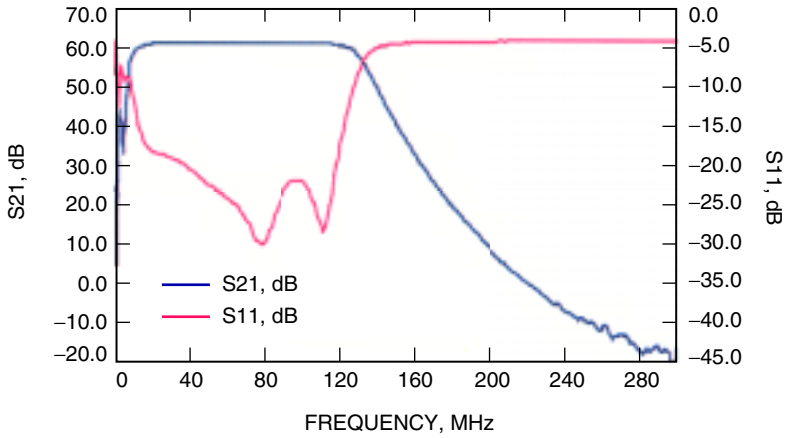

Fig. 7. Input return loss and gain of the downconverter IF section.

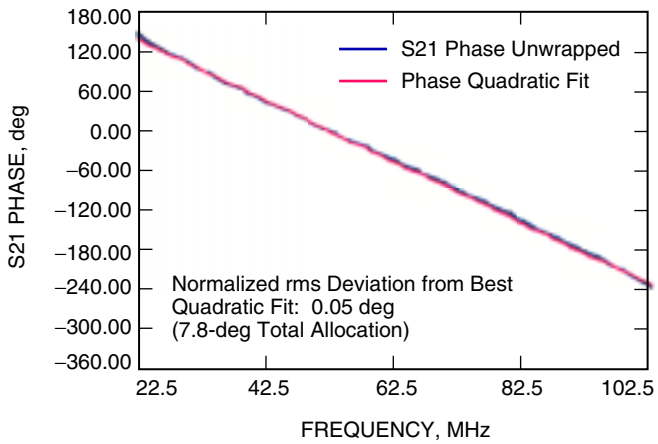

Fig. 8. Phase linearity of the downconverter IF section.

Table 1. L-band transceiver frequency response summary. Refer to Fig. 3 for port names.

Frequency response parameter	Value, dB	Notes
T/R_RF input to BB_out [max ripple]	1.20	—
T/R_RF input to BB_out [gain]	94.12	—
T/R_RF input to TP_3 [max ripple]	0.42	—
T/R_RF input to TP_3 [gain]	21.30	—
Chirp_in input to caltone_out [max ripple]	0.43	—
Chirp_in input to caltone_out [gain]	16.37	$P_{\text{in}} = -0.5$ dBm, $P_{\text{out}} = 15.87$ dBm, 1247.5 MHz HP8562A
Chirp_in input to TP_1 [gain]	−27.00	—
Chirp_in input to TP_2 [gain]	−47.33	$P_{\text{in}} = 0$ dBm, 1247.5 MHz HP8562A
Chirp_in input to T/R_RF [max ripple]	0.40	—
Chirp_in input to T/R_RF [gain]	15.08	$P_{\text{in}} = 0$ dBm, $P_{\text{out}} = 15.08$ dBm

With a chirp_in level of −10 dBm, we measured a test point (TP)_3 level of −11 dBm, which corresponds to −32 dBm at the input to the LNA. The corresponding T/R_RF level is +6 dBm. Therefore, the measured T/R switch isolation is 38 dB. Increasing the input chirp level further begins to saturate the receive chain. For the maximum chirp_in level of +3 dBm, we measure 16 dBm out of T/R_RF. The expected level at the LNA input, therefore, is −22 dBm, which is well below the maximum allowable input level for that device, which is −5 dBm. The level measured at TP_3 was −8 dBm, which corresponds to +14 dBm out of the post-amplifier (before the 22-dB coupler). The receiver (except for the LNA) is saturated, but the receiver components are protected from damage by the excellent isolation of the T/R switch. How quickly the receiver recovers from this saturation is discussed in Section III.E.

C. Receiver Gain Compression

Radar systems require linear receivers with a high 1-dB compression point to enable a high instantaneous dynamic range. This reduces the intermodulation products in the receiver band when several bright targets are reflecting from the scene. The receiver reaches the 1-dB compression point at an input signal level of −76 dBm and an output level of 17.5 dBm.

Table 2. Caltone output to receiver input isolation. Refer to Fig. 3 for port names.

Caltone output to receiver input isolation	Level	Isolation, dB
T/R_RF input to TP_3 [gain]	21.30 dB	—
T/R_RF input to BB_out [gain]	94.12 dB	—
142.5-MHz source at chirp_in	−40.00 dBm	—
Caltone_out	−22.00 dBm	—
TP_1	−65.00 dBm	—
TP_2	−85.67 dBm	—
TP_3	−97.83 dBm	Caltone_out − TP_3 + Gain (T/R_RF to TP_3) = 97
BB_out	−27.83 dBm	Caltone_out − BB_out + Gain (T/R_RF to BB_out) = 100
182.5-MHz source at chirp_in	−40.00 dBm	—
Caltone_out	−21.83 dBm	—
TP_1	−65.67 dBm	—
TP_2	−85.83 dBm	—
TP_3	−97.50 dBm	Caltone_out − TP_3 + Gain (T/R_RF to TP_3) = 97
BB_out	−27.33 dBm	Caltone_out − BB_out + Gain (T/R_RF to BB_out) = 100
222.5-MHz source at chirp_in	−40.00 dBm	—
Caltone_out	−22.17 dBm	—
TP_1	−68.00 dBm	—
TP_2	−85.83 dBm	—
TP_3	−98.50 dBm	Caltone_out − TP_3 + Gain (T/R_RF to TP_3) = 98
BB_out	−27.33 dBm	Caltone_out − BB_out + Gain (T/R_RF to BB_out) = 100

To measure the receiver output two-tone third-order intercept point, 1232-MHz and 1235-MHz signals of equal magnitudes were combined and input to the receiver. The first- and third-order products were measured. The output two-tone third-order intercept point (OTTIP) can be calculated as half the difference between the third-order product and the first-order product, plus the output level of the first-order product, in dBm. This test was repeated at three different signal levels to ensure the receiver was not in saturation. The results consistently indicated an OTTIP of 22.5 dBm.

D. LO Power Sensitivity

It is desirable to have low sensitivity to the LO power level in order to increase the amplitude and phase stability of the radar. This is particularly important in interferometry applications as well as in scatterometry. The effect of a change in LO power was measured for both the upconverter and the downconverter. The results are shown in Fig. 9, which indicates that a ±1-dB change in LO power results in minimal change in transmit and receive gain.

E. Switching Response (Speed and Recovery from Saturation)

Radar systems switch between transmit and receive at a pulse repetition frequency (PRF) on the order of several thousand pulses per second. We have designed the L-band transceiver to operate at a PRF up to 2 kHz. It is important that the receiver be able to recover from its saturated state, which is induced by the transmit pulse, in time for linear amplification of the return echo. Typically, this recovery time should be on the order of a microsecond. Using the test setup shown in Fig. 10, the dynamic performance of the transceiver RF switches was tested. Figure 11 shows the complementary outputs of the switch drivers (i.e., the control signal inputs to the RF switches) driven with a pulse generator. Note that

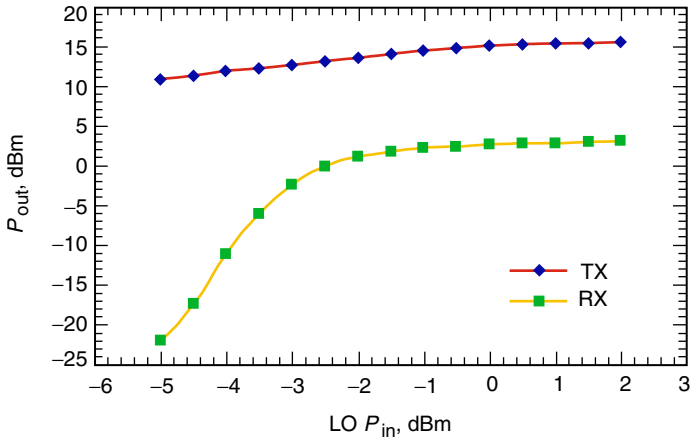

Fig. 9. LO sensitivity. The nominal LO input power level is 0 dBm.

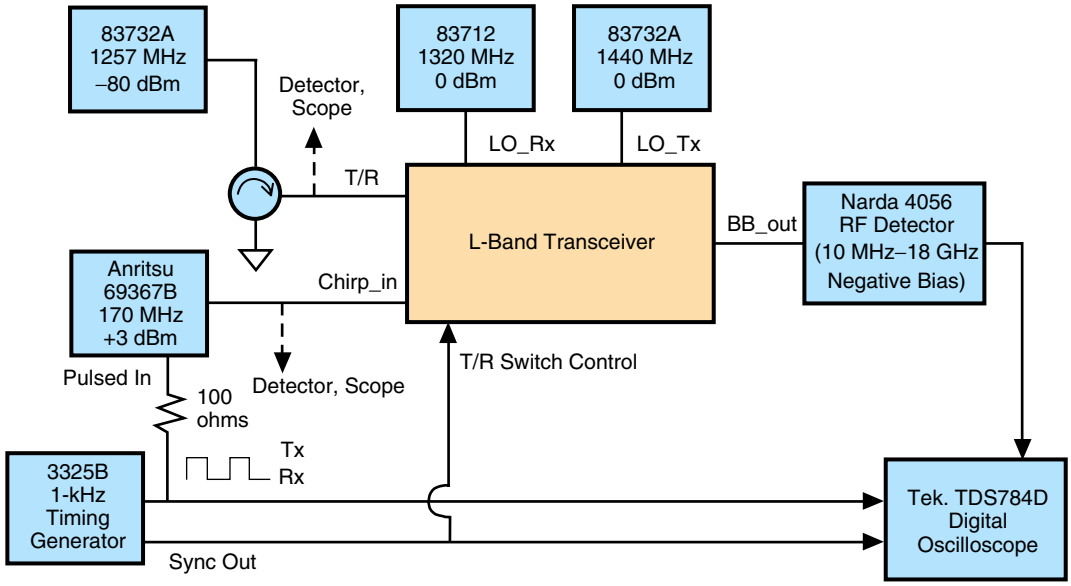

Fig. 10. Transmit saturation switch recovery test setup.

channel (Ch) 4 in Fig. 11 has a fall time of roughly 2.2 μs caused from 4000-pF capacitors that were used to filter control signals to the RF switches. The switch control signal can achieve ground potential quickly but has a long time constant, resulting in a relatively slow recovery time. The switch recovery time can be easily reduced in the next design iteration by using dedicated switch drivers for each switch control input and by using high-speed filtering components.

In Fig. 12, we see the transceiver switch transition from transmit mode to receive mode (channel 3 going from high to low) and the corresponding detected baseband signal at the receiver output (channel 1). A residual transmit leakage signal, which was not completely quenched by the pulse modulation, is amplified by the 94-dB gain receiver and is present during the receive window. This leakage signal provides a "test signal" to observe recovery from saturation. We observed about 2 μs of transients while the switches were transitioning (this can be improved considerably, as explained above). After about 2 μs, most of the switch isolation should be achieved (a separate test showed that, when the control voltage reaches 2.5 V, isolation is almost nominal). Another 1.5 μs are required for the receiver to fully recover from

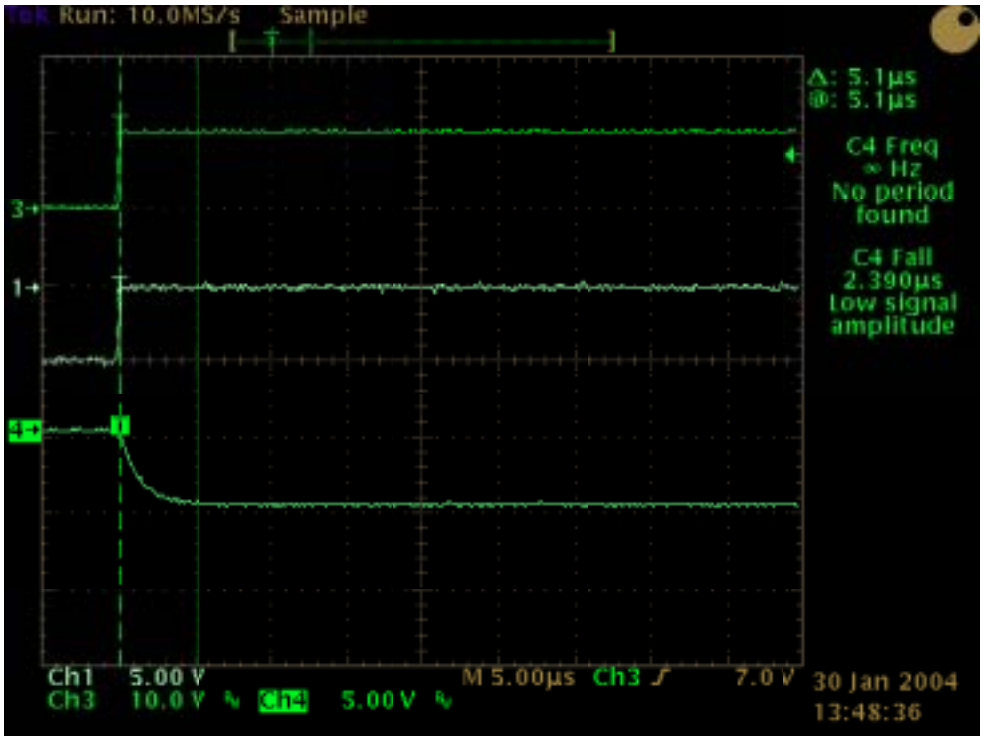

Fig. 11. Pulse generator rising edge into transceiver switch control input (Ch 3). Transceiver (internal) complementary RF switch drive signals (Ch 1 and Ch 4).

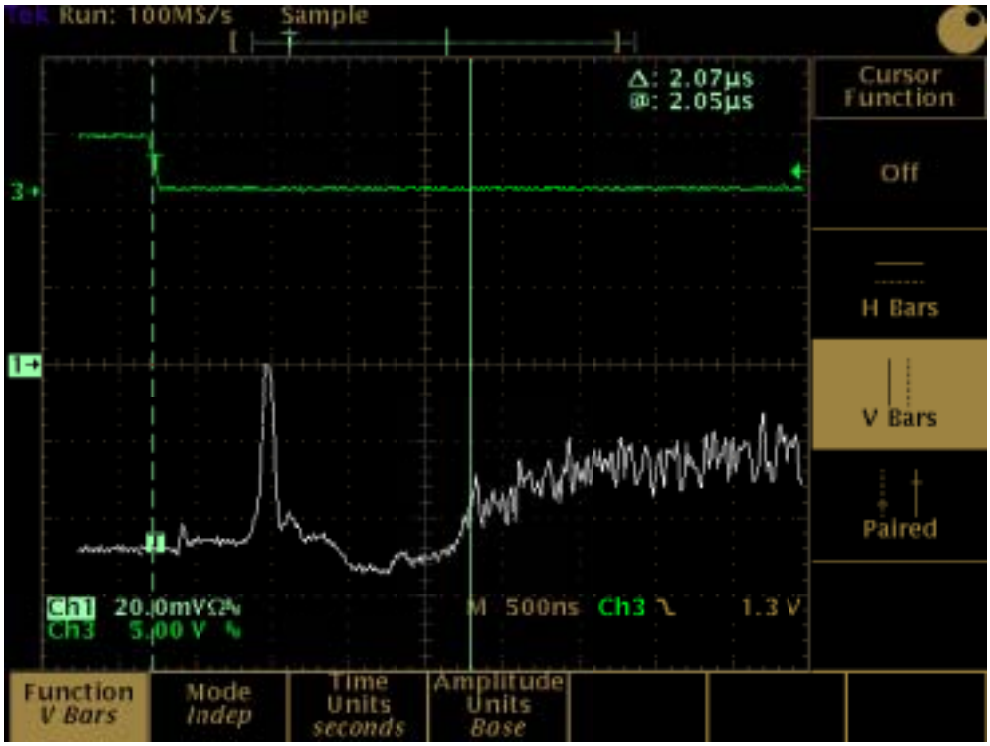

Fig. 12. Pulse generator falling edge into transceiver switch control input (Ch 3). RF detector output of transceiver BB output, showing recovery from saturation due to transmit event (Ch 1).

saturation to full gain. Therefore, the total time for the receiver to recover from switching transients and saturation due to the transmit event is roughly 4 μs. The recovery time would be taken into account in the design of the radar receive-window-position timing; however, typically the receive window is several hundred microseconds long, so a few microseconds of recovery time pose no significant limitation.

F. Receiver Noise Figure

The noise figure of a radar system determines its signal-to-noise ratio (SNR) when traded off against transmit power. However, since the radar is looking down at the planet, its system temperature does not need to be significantly better than the noise temperature contributed by the scene. The noise figure of the radar system is determined by the front-end T/R module. Our transceiver is downstream from the T/R module and so does not necessarily need a noise figure better than 5 dB.

The noise figure was measured at room temperature using the Agilent noise figure measurement system. As can be seen from Fig. 13, the receiver front-end noise figure and gain are as expected when measured at the TP_3 output: 42 dB (LNAs) − 22 dB (coupler) = 20 dB of gain and a noise figure of 3.5 dB. However, as can be seen from Fig. 14, when performing the measurement at the baseband output (BB_out), to include the downconversion in frequency, we measure an increase of about 3 dB in noise figure. Ideally, the noise figure would increase only by a small fraction of a dB when adding receiver stages. To understand this significant degradation, we first look at the fact that we have only about 10-dB rejection in our RF bandpass filter (BPF) at the fold-over frequency (i.e., the edge of our downconverted band: 22.5 MHz). This would allow some of the wideband noise from the test-set noise diode to alias into our measurement. This effect would manifest itself as a 0.4-dB increase in noise figure at one end of the band, decreasing to a 0.04-dB increase at the 102.5-MHz end of the band. This phenomenon is not a problem because we don't expect a wideband signal to come into the radar (our signal is band limited).

Next we look at the noise contribution of the LNAs that are between the bandpass filter and the mixer. They are very wide band. Their noise level outside our band is only 1-dB lower than the in-band noise. So, when their out-of-band noise folds into the mixer, the resultant increase in noise figure is 1.7 dB. There also may be some harmonics and energy due to mismatch of the out-of-band noise that could increase these theoretical contributions further.

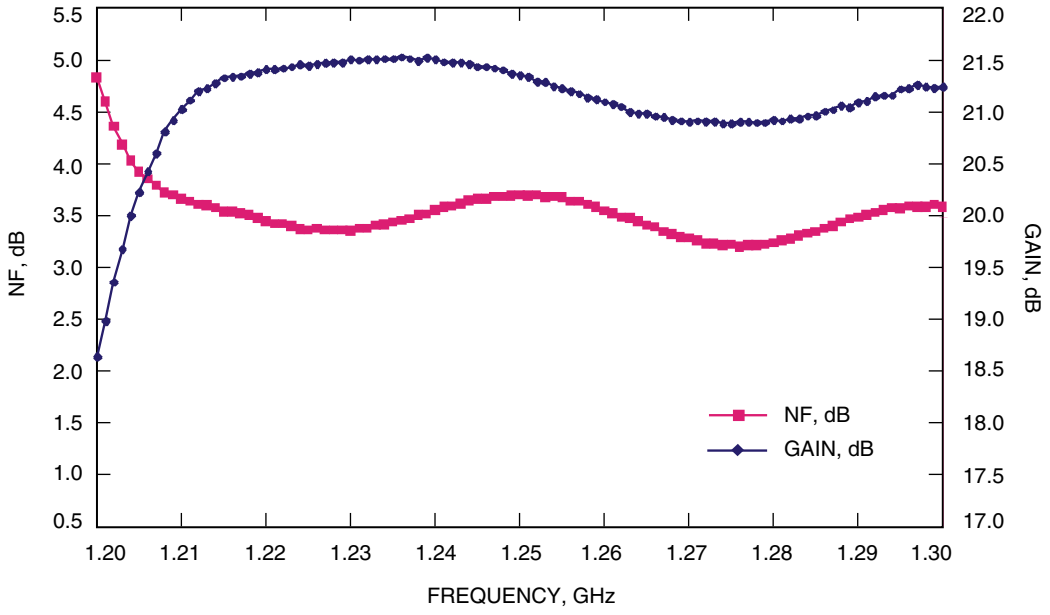

Fig. 13. Receiver front-end noise figure and gain to TP_3 output. (From J. Fernandez, January 12, 2004, Agilent noise figure measurement system.)

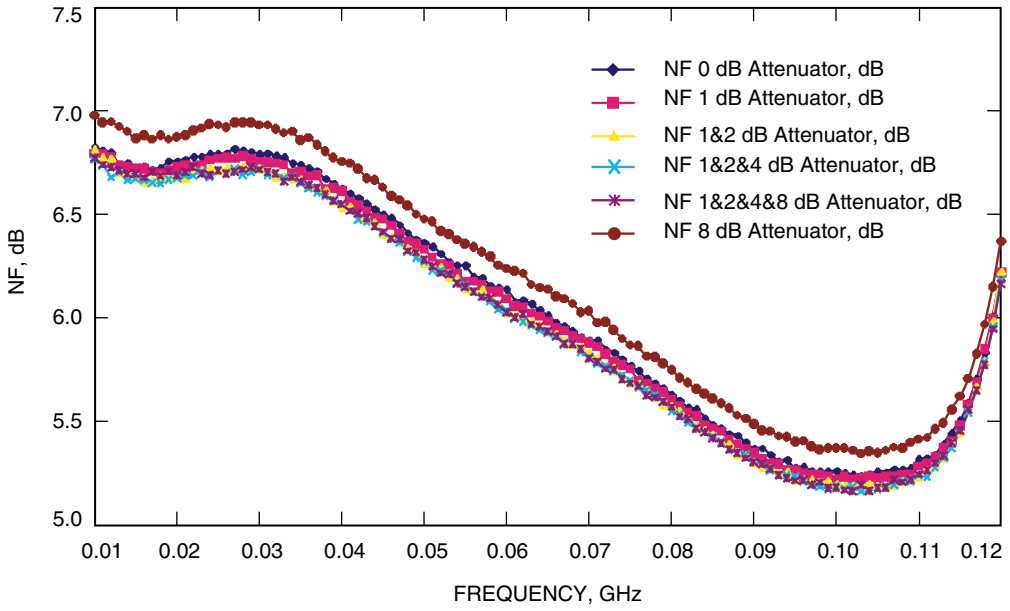

Fig. 14. Downconverter noise figure to BB_out. (From J. Fernandez, January 12, 2004, Agilent noise figure measurement system.)

In a future implementation, if the noise figure is critical, this problem can be solved easily by placing another BPF just before the mixer. For this implementation, the priority was on miniaturization, so an additional filter was not used. The filter position was chosen to be in front of the LNA in order to protect from strong out-of-band RFI signals that could saturate the receiver. Since a low-noise T/R module typically will precede the receiver, this degradation in NF should not have a significant impact on overall system performance.

IV. Summary and Conclusions

Table 3 summarizes the key performance parameters of the miniature radar electronics L-band transceiver. While this component is intended to be an element of the miniaturized radar electronics module under development, it also can be adapted to any number of radar applications due to its flexible design architecture. The performance meets or exceeds requirements in gain, isolation, dynamic range, and linearity. In areas where performance fell short, such as noise figure and switch recovery, the problem is well understood and easy to fix in the next iteration. The work done for this task was accomplished with very modest resources and in only one iteration for design, board layout, and housing machining. The results suggest that the design architecture, techniques, materials, and components are appropriate candidates for the next space-flight radar missions, with promise of reduced risk as well as reduced power, mass, and size. The design is flexible, and variations can be incorporated without incurring significant risk.

Table 3. Up-/down-converter performance summary.

Parameter	Value	Notes
Module		
Mass	270 g	—
Dimensions	$15.5 \times 6 \times 2.2$ cm	—
Power dissipation	3 W	Can be improved by changing DC supply/control filtering design
Power supplies	—	+8 V at 365 mA, −8 V at 7 mA, 5 V at 1 mA
Bandwidth	80 MHz	—
Center frequency	1257.5 MHz	—
Tx to Rx switch recovery time	3 μs	Can be improved by changing switch control filtering
Upconverter		
IF input cente frequency	182.5 MHz	—
IF input level	0 dBm	—
RF output	15.5 dBm	—
Passband ripple	0.4 dB	—
LO frequency	1440 MHz	—
LO input level	0 dBm	—
Downconverter		
Output IF center frequency	62.5 MHz	—
Gain	94 dBm	Max gain
Programmable attenuator range	15 dB	1-dB steps
Output 1-dB compression	17.5 dBm	—
Output two-tone third-order intercept	22.5 dBm	—
Noise figure	7 dB	Can be 4 dB if a duplicate filter is placed at mixer input
Caltone output to receiver input isolation	97 dB	—
Passband ripple	1.2 dB	Can be improved by incorporating matching networks between components
LO frequency	1320 MHz	—
LO input level	0 dBm	—

Acknowledgments

The design and development of the L-band transceiver module was sponsored by JPL's Research and Technology Development Program. The testing of the module was funded by the InSAR Technology Development Task sponsored by the Earth Science Enterprise. Special thanks to Tony DeKorte, Mary Wells, Carolina Flores-Helizon, and Chi Truong for their excellent support in assembly of the module.

Reference

[1] J. C. Curlander and R. N. McDonough, *Synthetic Aperture Radar, Systems and Signal Processing*, New York: John Wiley and Sons, Inc., pp. 256–261, 1991.